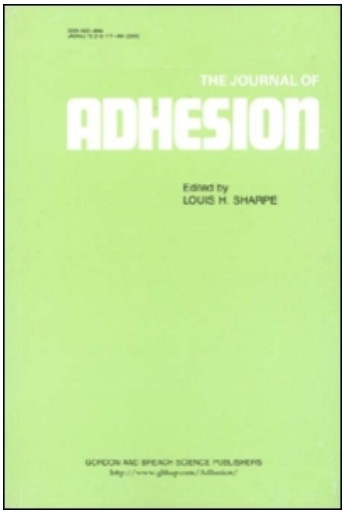

The Journal of Adhesion
Publication details, including instructions for authors and subscription information:
http://www.informaworld.com/smpp/title~content=t713453635

Van der Waals Attraction in Multilayer Structures

Dieter Langbein[a]
[a] Battelle-Institut e. V., Frankfurt/Main, Germany

To cite this Article Langbein, Dieter(1972) 'Van der Waals Attraction in Multilayer Structures', The Journal of Adhesion, 3: 3, 213 — 235
To link to this Article: DOI: 10.1080/00218467208072194
URL: http://dx.doi.org/10.1080/00218467208072194

J. Adhesion, 1972, Vol. 3, pp. 213–235

Printed in Northern Ireland

Van der Waals Attraction in Multilayer Structures

DIETER LANGBEIN

Battelle-Institut e.V., Frankfurt/Main, Germany

(*Received March* 20 1971)

Abstract

The dispersion energy between multilayer systems is calculated from the energy of the electromagnetic field fluctuations, which originate in the interspace and are repeatedly reflected or transmitted by all interfaces. The resulting energy terms are summed explicitly for the case of a periodic double layer by means of combinatorial analysis. The dispersion energy between different layers turns out to be of longer range than that resulting from a pairwise integration of d^{-6} interactions, on account of the large number of additional reflection terms. The reflection terms of order $l \geq 5$ even show extremes in their dependence on the separation a_2. However, their generally decreasing weight makes it very unlikely that these extremes might also be encountered in the dispersion energy.

1 INTRODUCTION

Recently, a method was derived, which enables a calculation of the non-retarded dispersion energy between macroscopic bodies from their macroscopic reaction fields[1,2]. The application of this method to the attraction between two spheres makes it possible to represent their mutual dispersion energy by a Taylor series with respect to the reduced radii. This series can be summed exactly by using appropriate upper or lower bounds for the dielectric constants involved[2,3].

Another geometrically simple system in which van der Waals attraction plays an important role for cohesion is the multilayer structure. This applies to the attraction between different layers of a layer lattice, the attraction between different crystallic regions in polymers and the attraction between different layers of biological structures. Calculations of van der Waals attraction in multilayer systems have recently been reported by Ninham and Parsegian[4,5]. From the Lifshitz theory[6,7] they find the attraction between

different layers to be non-additive and of longer range than expected from a pairwise integration of d^{-6} interactions between the individual molecules.

Compared to the Lifshitz theory the present procedure is more lucid and straightforward. We start by calculating the reaction potential of an infinite layer system caused by an external point charge. This potential is described in terms of image charges, *i.e.* by an infinite number of reflection and transmission potentials with respect to the different layer boundaries. The dispersion energy between two such layer structures, which is the integral over the fluctuation fields times the reaction fields of both systems, is obtained by summation over all closed sequences of reflections and transmissions, which connect the two interacting partners. We carry out this summation explicitly for periodic double layer systems. Owing to the increased number of field reflections, the dispersion energy across a single layer turns out to be of longer range than that between attracting half-spaces. Numerical results are reported.

The direct correspondence between each term of the final energy expression and a discrete sequence of reflections and transmissions enables us to extend the present method to include retarded interactions.

II REACTION POTENTIALS

The basis of our calculations is the fact that the dispersion energy between two macroscopic bodies A and B can be represented in the form[1]

$$\Delta E_{AB} = -\frac{\hbar}{4\pi}\int_{-\infty}^{+\infty} d\omega \left\{ \sum_{i\varepsilon A}\sum_{j\varepsilon B} \alpha_i T_{ij}^{scr} \alpha_j T_{ji}^{scr} + \frac{1}{2}\sum_{i,k\varepsilon A}\sum_{j,l\varepsilon B} \alpha_i T_{ij}^{scr}\alpha_j T_{jk}^{sc\varepsilon}\alpha_k T_{kl}^{scr}\alpha_l T_{li}^{scr} + \cdots \right\} \tag{1}$$

where T_{ij}^{scr} is the screened field of a dipole i in A at position j outside A. If we replace body B by its macroscopic reaction field

$$S_{ik} = \sum_{j\varepsilon B} \alpha_i T_{ij}^{scr} \alpha_j T_{ji}^{scr} \tag{2}$$

we are left with an integration within body A[1],

$$\Delta E_{AB} = -\frac{\hbar}{4\pi}\int_{-\infty}^{+\infty} d\omega \left\{ \sum_{i\varepsilon A} S_{ii} + \frac{1}{2}\sum_{i,k\varepsilon A} S_{ik}S_{ki} + \cdots \right\} \tag{3}$$

The first sum in (3) contains the direct reaction of body B to a field fluctuation at i in A, the second term describes the interaction via polarization of positions k in A, and so on.

If body B is a half-space with dielectric constant ε_1 (Figure 1), we can describe its reaction potential due to an external point charge q at position $\mathbf{0}$

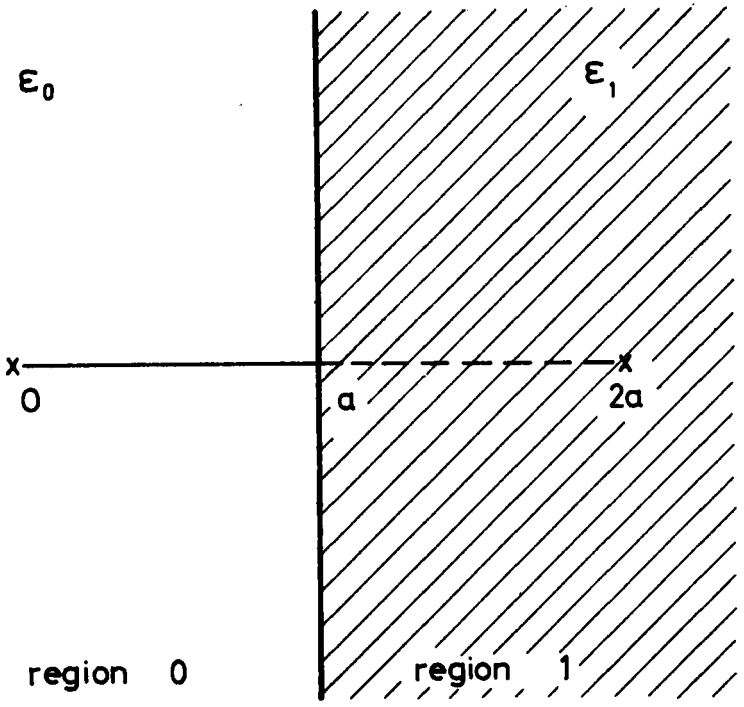

FIGURE 1 Half-space

by an image charge $q(\varepsilon_0 - \varepsilon_1)/(\varepsilon_0 + \varepsilon_1)$ at position $2\mathbf{a}$. The total exterior potential ϕ_0 (region 0) is

$$4\pi\varepsilon_o\phi_o = \frac{q}{|\mathbf{r}|} + \frac{\varepsilon_o - \varepsilon_1}{\varepsilon_o + \varepsilon_1}\frac{q}{|\mathbf{r} - 2\mathbf{a}|} \tag{4}$$

whereas in the interior of the half-space (region 1) we obtain

$$4\pi\varepsilon_1\phi_1 = \frac{2\varepsilon_1}{\varepsilon_o + \varepsilon_1}\frac{q}{|\mathbf{r}|} \tag{5}$$

If instead of a half-space we consider the infinite layer system shown in Figure 2, we have to satisfy additional steadiness conditions for ϕ_1 at the interface f_{12} between regions 1 and 2: we have to add the potential of an

image charge $q_1(\varepsilon_1 - \varepsilon_2)/(\varepsilon_1 + \varepsilon_2)$ at position $2(\mathbf{a} + \mathbf{a}_1)$, where $q_1/q = 2\varepsilon_1/(\varepsilon_0 + \varepsilon_1)$.

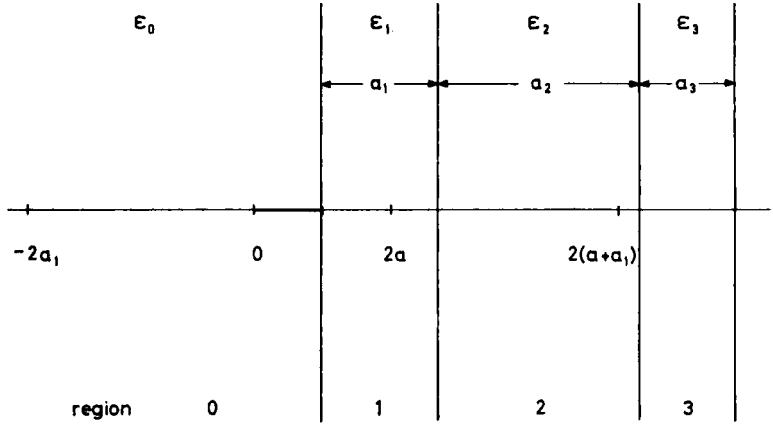

FIGURE 2 Infinite layer system

This, in turn, violates the steadiness of ϕ_1 at the interface f_{01} between regions 0 and 1: we have to continue the potential of the image charge at position $2(a + a_1)$ to region 0 and to add the potential of an image charge at $-2a_1$ in region 1.

For a construction of the external potential ϕ_0 in general order we note the following scheme:

(a) The steadiness conditions for ϕ_n at the interface f_{nn+1} require addition of its reflection potential with the weight factor $(\varepsilon_n - \varepsilon_{n+1})/(\varepsilon_n + \varepsilon_{n+1})$ in region n and transmission of ϕ_n with the weight factor $2\varepsilon_{n+1}/(\varepsilon_n + \varepsilon_{n+1})$ to region n + 1.

(b) Reflections and transmissions of the potential of this type are represented by the diagrams shown in Figure 3, with the respective weight given on the right.

(c) Each contribution to the external potential ϕ_0 corresponds to a closed sequence of reflections and transmissions of the unscreened potential at the interfaces f_{nn+1}.

(d) We find all contributions to ϕ_0 by constructing all paths from the diagrams shown in Figure 3, which start and end in the exterior (region 0). The weight of these contributions is the product of the weights of the corresponding diagrams. The position of the image charge is the sum over the diagram lengths.

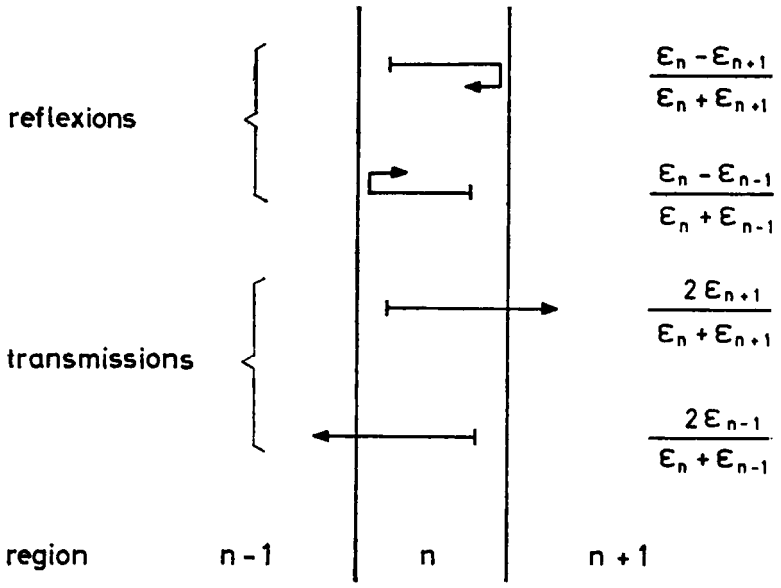

FIGURE 3 Diagrams

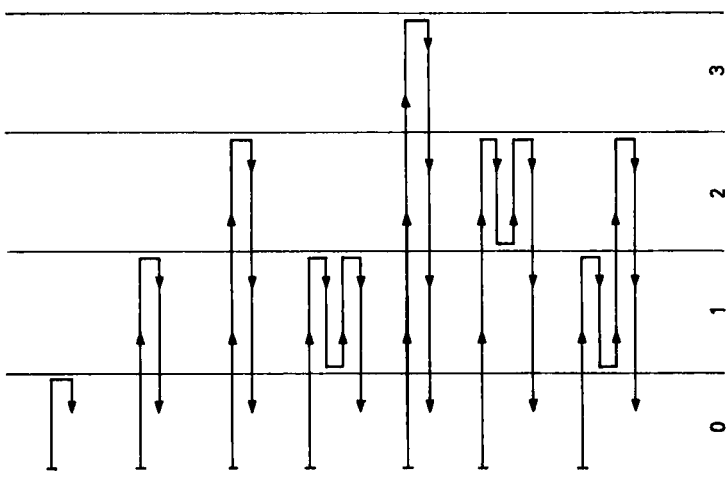

FIGURE 4 Reaction potential

This is done explicitly in Figure 4. We find the reaction potential of an infinite layer system due to an external point charge q to be

$$4\pi\varepsilon_o \Delta\phi_0 = q \left\{ \frac{\varepsilon_0 - \varepsilon_1}{\varepsilon_0 + \varepsilon_1} \frac{1}{|\mathbf{r} - 2\mathbf{a}|} + \frac{4\varepsilon_0\varepsilon_1}{(\varepsilon_0 + \varepsilon_1)^2} \frac{\varepsilon_1 - \varepsilon_2}{\varepsilon_1 + \varepsilon_2} \frac{1}{|\mathbf{r} - 2\mathbf{a} - 2\mathbf{a}_1|} + \frac{4\varepsilon_0\varepsilon_1}{(\varepsilon_0 + \varepsilon_1)^2} \frac{4\varepsilon_1\varepsilon_2}{(\varepsilon_1 + \varepsilon_2)^2} \frac{\varepsilon_2 - \varepsilon_3}{\varepsilon_2 + \varepsilon_3} \frac{1}{|\mathbf{r} - 2\mathbf{a} - 2\mathbf{a}_1 - 2\mathbf{a}|} + \cdots \right\} \tag{6}$$

The multilayer shown in Figure 2 reacts to an external point charge like an infinite set of independent half-spaces with appropriately adapted dielectric constants at distances $\mathbf{a} + \Sigma n_i \mathbf{a}_i$, n_i integer.

III DISPERSION ENERGY

In order to calculate the dispersion energy between the two multilayer systems A and B shown in Figure 5, we have to calculate the screened external field T_{ij}^{scr} of dipole i in A and the respective reactions field S_{ik} of body B, and to carry out the integration (3) over body A.

We may construct the screened external potential of a point charge q at i in A by successive reflections and transmissions of the direct potential at all interfaces f_{nn+1} of A, *i.e.* by a diagram technique equivalent to that introduced

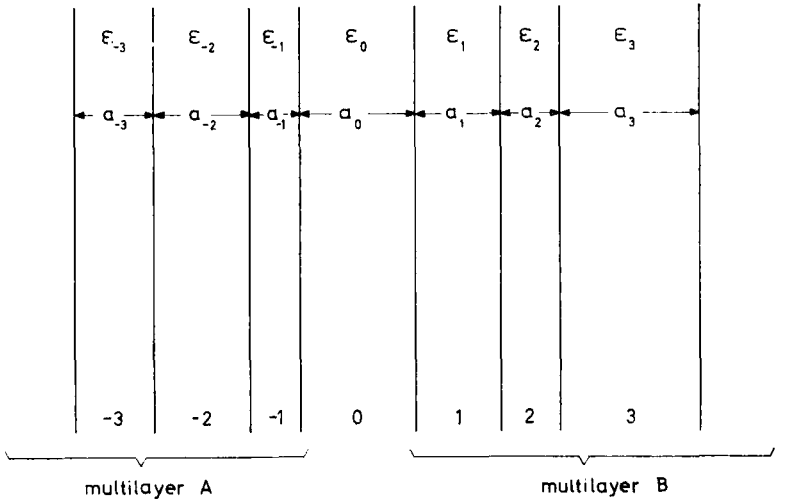

FIGURE 5 Multilayers A and B

in section 2. We obtain the potential of an infinite set of point charges, which, in turn, serves as a basis for the construction of the reaction potential of B according to (6). The latter is the sum over the potentials of all successive image charges in B. This additive structure is maintained in the two final steps of the calculation of the dispersion energy (3). We have to differentiate the reaction potential with respect to the origin $\mathbf{r}i$ and with respect to the test point $\mathbf{r}_k$ in order to obtain the reaction field S_{ik} of B due to dipole i in A, and to carry out the integrations required in (3). The dispersion energy ΔE_{AB} between the two multilayers A and B is additively composed of that between infinite sets of half-spaces with appropriately adapted dielectric constants at separations $\Sigma n_i \mathbf{a}_i$, n_i integer.

Having found the analytic structure of ΔE_{AB}, we may reduce the above calculations by first assuming A to be a half-space ($\mathbf{a}_{-1} \to \infty$), and then adding the effect of the layers $-2, -3, \ldots$ on account of symmetry arguments.

If A is a half-space and B is a half-space, we know from previous investigations[1,2] that the dispersion energy per unit surface area is given by

$$\Delta E_{AB} = -\frac{\hbar}{16\pi^2 a_0^2} \int_{-\infty}^{+\infty} d\omega \sum_{l=1}^{\infty} \frac{1}{l^3} \left(\frac{\varepsilon_0 - \varepsilon_{-1}}{\varepsilon_0 + \varepsilon_{-1}} \frac{\varepsilon_0 - \varepsilon_1}{\varepsilon_0 + \varepsilon_1} \right)^l \tag{7}$$

Eq. (7) is identical with the Lifshitz formula for the non-retarded limit[6]. The summation index l counts the number of field reflections between A and B.

Since B, rather than being a half-space, is a multilayer reacting with the potential given by (6), we have to take into account the full system of point charges (6) each time the field touches B. We obtain in first order of reflection ($l = 1$)

$$\Delta_1 E_{AB} = -\frac{\hbar}{16\pi^2} \int_{-\infty}^{+\infty} d\omega \frac{\varepsilon_0 - \varepsilon_{-1}}{\varepsilon_0 + \varepsilon_{-1}} \left\{ \frac{\varepsilon_0 - \varepsilon_1}{\varepsilon_0 + \varepsilon_1} \frac{1}{a_0^2} + \frac{4\varepsilon_0 \varepsilon_1}{(\varepsilon_0 + \varepsilon_1)^2} \frac{\varepsilon_1 - \varepsilon_2}{\varepsilon_1 + \varepsilon_2} \frac{1}{(a_0 + a_1)^2} + \cdots \right\} \tag{8}$$

and in second order of reflection ($l = 2$)

$$\Delta_2 E_{AB} = -\frac{\hbar}{32\pi^2} \int_{-\infty}^{+\infty} d\omega \left(\frac{\varepsilon_0 - \varepsilon_{-1}}{\varepsilon_0 + \varepsilon_{-1}} \right)^2 \left\{ \left(\frac{\varepsilon_0 - \varepsilon_1}{\varepsilon_0 + \varepsilon_1} \right)^2 \frac{1}{(2a_0)^2} + 2 \frac{\varepsilon_0 - \varepsilon_1}{\varepsilon_0 + \varepsilon_1} \frac{4\varepsilon_0 \varepsilon_1}{(\varepsilon_0 + \varepsilon_1)^2} \frac{\varepsilon_1 - \varepsilon_2}{\varepsilon_1 + \varepsilon_2} \frac{1}{(2a_0 + a_1)^2} + \cdots \right\} \tag{9}$$

Each term in (8) corresponds to a path as shown in Figure 4, which is closed by a reflection at the surface f_{-10} of A. Each term in (9) corresponds to a combination of two paths as shown in Figure 4, which is closed by two reflections at the surface f_{-10} of A.

Since A is not a half-space, but a multilayer too, we now include the effect of this multilayer for reasons of symmetry. Whenever the field touches A, a full set of point charges similar to that given by (6) must become active. We have to replace the reaction potential of half-space A by that of multilayer A. This yields the following diagram technique for ΔE_{AB}.

We find all contributions to the dispersion energy between the multilayers A and B by drawing all closed paths consisting of diagrams as shown in Figure 3, which touch A and B at least once. The weight of these contributions is the product of the weights of the corresponding diagrams. The effective separation entering the dispersion energy is one half the sum over the diagram lengths. Graphs consisting of l equivalent parts receive the additional weight factor $1/l$ in order to avoid multiple counting.

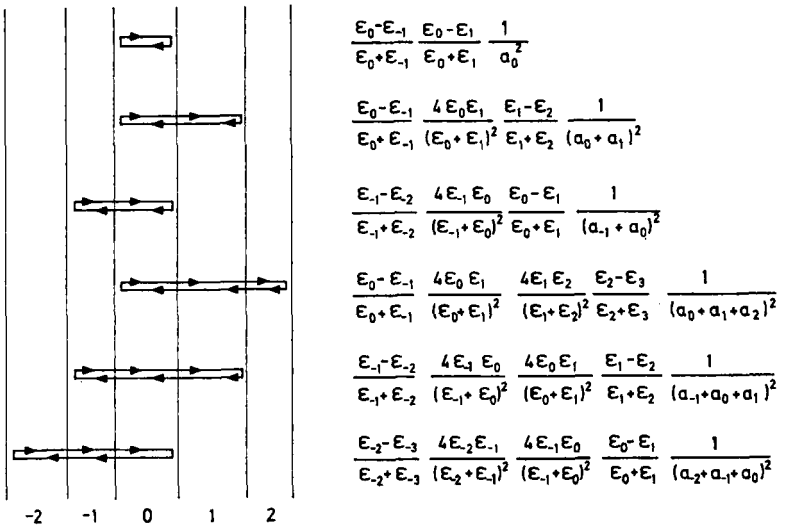

FIGURE 6 Contributions to ΔE_{AB}, two reflections

This diagram technique is demonstrated explicitly in Figure 6 and 7. We wind up with

$$\Delta E_{AB} = -\frac{\hbar}{16\pi^2}\int_{-\infty}^{+\infty} d\omega \left\{ \frac{\varepsilon_0-\varepsilon_{-1}}{\varepsilon_0+\varepsilon_{-1}}\frac{\varepsilon_0-\varepsilon_1}{\varepsilon_0+\varepsilon_1}\frac{1}{a_0^2} + \frac{\varepsilon_0-\varepsilon_{-1}}{\varepsilon_0+\varepsilon_{-1}}\frac{4\varepsilon_0\varepsilon_1}{(\varepsilon_0+\varepsilon_1)^2}\frac{\varepsilon_1-\varepsilon_2}{\varepsilon_1+\varepsilon_2}\frac{1}{(a_0+a_1)^2} + \cdots \right\} \quad (10)$$

The diagram technique described here is consistent with our ideas on the origin of van der Waals attraction. We have to calculate the energy change of

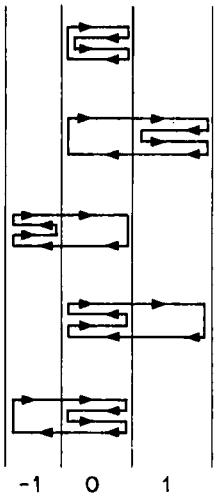

$$\frac{1}{2}\left(\frac{\varepsilon_0-\varepsilon_{-1}}{\varepsilon_0+\varepsilon_{-1}}\right)^2\left(\frac{\varepsilon_0-\varepsilon_1}{\varepsilon_0+\varepsilon_1}\right)^2\frac{1}{(2a_0)^2}$$

$$\frac{\varepsilon_0-\varepsilon_{-1}}{\varepsilon_0+\varepsilon_{-1}}\frac{4\varepsilon_0\varepsilon_1}{(\varepsilon_0+\varepsilon_1)^2}\left(\frac{\varepsilon_1-\varepsilon_2}{\varepsilon_1+\varepsilon_2}\right)^2\frac{\varepsilon_1-\varepsilon_0}{\varepsilon_1+\varepsilon_0}\frac{1}{(a_0+2a_1)^2}$$

$$\frac{\varepsilon_{-1}-\varepsilon_0}{\varepsilon_{-1}+\varepsilon_0}\left(\frac{\varepsilon_{-1}-\varepsilon_{-2}}{\varepsilon_{-1}+\varepsilon_{-2}}\right)^2\frac{4\varepsilon_{-1}\varepsilon_0}{(\varepsilon_{-1}+\varepsilon_0)^2}\frac{\varepsilon_0-\varepsilon_1}{\varepsilon_0+\varepsilon_1}\frac{1}{(2a_{-1}+a_0)^2}$$

$$\frac{\varepsilon_0-\varepsilon_1}{\varepsilon_0+\varepsilon_1}\left(\frac{\varepsilon_0-\varepsilon_{-1}}{\varepsilon_0+\varepsilon_{-1}}\right)^2\frac{4\varepsilon_0\varepsilon_1}{(\varepsilon_0+\varepsilon_1)^2}\frac{\varepsilon_1-\varepsilon_2}{\varepsilon_1+\varepsilon_2}\frac{1}{(2a_0+a_1)^2}$$

$$\frac{\varepsilon_{-1}-\varepsilon_{-2}}{\varepsilon_{-1}+\varepsilon_{-2}}\frac{4\varepsilon_{-1}\varepsilon_0}{(\varepsilon_{-1}+\varepsilon_0)^2}\left(\frac{\varepsilon_0-\varepsilon_1}{\varepsilon_0+\varepsilon_1}\right)^2\frac{\varepsilon_0-\varepsilon_{-1}}{\varepsilon_0+\varepsilon_{-1}}\frac{1}{(2a_0+a_{-1})^2}$$

FIGURE 7 Contributions to ΔE_{AB}; four reflections

the field fluctuations crossing region 0. An electromagnetic wave originating in region 0 undergoes reflections and transmissions at all interfaces $f_{i\,i+1}$, where the dielectric properties of the surrounding media change. Each return of the wave to region 0 entails a change of its energy. An extension of the present method to include retardation is obvious.

IV PERIODIC DOUBLE LAYERS

The diagram technique developed in section 3 provides us with the full expression for the dispersion energy between arbitrary multilayers. As long as we do not require special symmetry, we can merely sum up the resulting series numerically.

A system especially suited to an analytical summation of most contributions is the periodic double layer shown in Figure 8. We want to calculate the dispersion energy across region 0, and thus consider regions 1, 2, 3, . . . to form multilayer B and regions -1, -2, -3, . . . to form multilayer A. All effective separations in the final expression for ΔE_{AB} assume the form $ma_1 + na_2$. It is merely a question of combinatorial analysis to sum up all contributions yielding the same separation. With respect to the dielectric factors involved, we note from Figures 6 and 7 that only two different factors, namely $(\varepsilon_1 - \varepsilon_2)/(\varepsilon_1 + \varepsilon_2)$ and $4\varepsilon_1\varepsilon_2/(\varepsilon_1 + \varepsilon_2)^2$ occur, the latter being equal to one minus the former. Thus, all dielectric terms entering the

dispersion energy can be expressed by the integrals

$$\Omega_l = \int_{-\infty}^{+\infty} d\omega \left(\frac{\varepsilon_1 - \varepsilon_2}{\varepsilon_1 + \varepsilon_2}\right)^{2l} \tag{11}$$

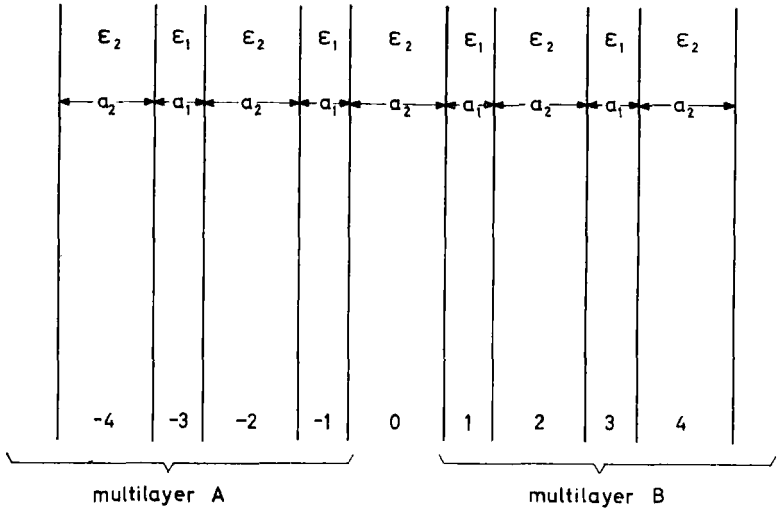

FIGURE 8 Periodic double layer

These are the integrals already involved in the dispersion energy (7) between two half-spaces. We expect the final expression for the dispersion energy between the multilayers shown in Figure 8 to have the form

$$\Delta E_{AB} = -\frac{\hbar}{16\pi^2} \sum_{l,m,n} A_{lmn} \frac{\Omega_l}{(ma_1 + na_2)^2} \tag{12}$$

with the coefficients A_{lmn} being combinatorial numbers.

We start the analysis of the coefficients A_{lmn} conveniently with the case $l = 1$, that is with the coefficients of the largest integral Ω_1. Since each reflection yields an additional factor $\pm(\varepsilon_1 - \varepsilon_2)/(\varepsilon_1 + \varepsilon_2)$, we obtain terms contributing to Ω_1 only from the unfolded paths shown in Figure 6. If such an unfolded path crosses n layers a_2, it may cross $n - 1$, n or $n + 1$ layers a_1, and may assume n different positions relative to region 0 (see Figure 9). We find the total contribution of these paths to be

$$\sum_{n=1}^{\infty} \binom{n}{1} \sum_{m=n-1}^{n+1} (-1)^{m-n+1} \binom{2}{m-n+1} \frac{1}{(ma_1 + na_2)^2} \times \left\{\Omega_1 - \binom{m+n-1}{1}\Omega_2 + \binom{m+n-1}{2}\Omega_3 \mp \cdots\right\} \tag{13}$$

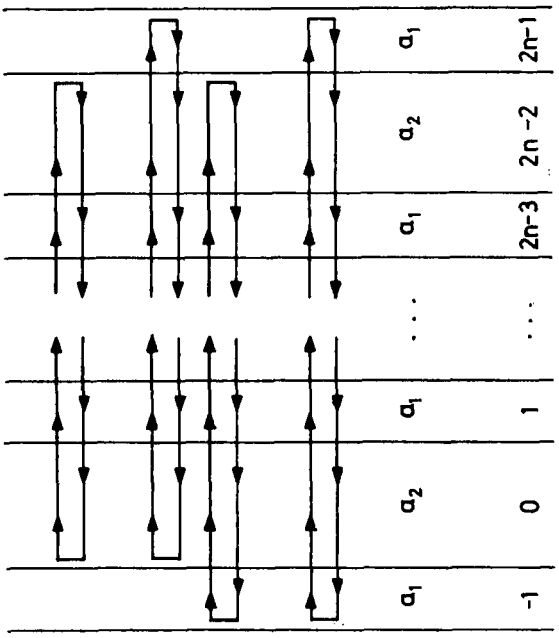

FIGURE 9 Paths containing two reflections

Since no other paths yield contributions to Ω_1, we conclude

$$A_{1mn} = (-1)^{m-n+1}\binom{2}{m-n+1}\binom{n}{1} \tag{14}$$

Further contributions to the second largest integral Ω_2 result only from paths containing four reflections, viz. the paths shown in Figure 7. If such a path crosses n layers a_2, it may cross $n-2$, $n-1$, n, $n+1$ or $n+2$ layers a_1. We distinguish three types:

(a) All paths, which cross region 0 twice, result from enlarging path I in Figure 10 for $n-2$ diagrams a_1+a_2 at the intersections 1, 2, 3, 4, Path Ia is derived by adding 1, 0, 2, 1 diagrams a_1+a_2 at 1, 2, 3, 4. We can then distribute up to four diagrams a_1 to the four ends 1, 2, 3, 4, see for instance path Ib. For the total contribution of these paths we find

$$\frac{1}{2}\sum_{n=2}^{\infty}\binom{n+1}{3}\sum_{m=n-2}^{n+2}(-1)^{m-n+2}\binom{4}{m-n+2}\frac{1}{(ma_1+na_2)^2} \times\left\{\Omega_2-\binom{m+n-2}{1}\Omega_3\pm\cdots\right\} \tag{15}$$

(b) Most paths, which cross region 0 only once, result from enlarging paths II in Figure 10 for $n-3$ diagrams a_1+a_2 at the intersections 1, 2, 3, 4 (path IIa). Having subsequently distributed up to four diagrams a_1 to the four ends 1, 2, 3, 4 (path IIb), we find the total contribution of these paths to be

$$2\sum_{n=3}^{\infty}\binom{n}{3}\sum_{m=n-2}^{n+2}(-1)^{m-n+2}\binom{4}{m-n+2}\frac{1}{(ma_1+na_2)^2} \times\left\{\Omega_2-\binom{m+n-2}{1}\Omega_3\pm\cdots\right\} \tag{16}$$

(c) A third type of paths crosses no region a_2 twice, see path III in Figure 10. These paths make the contribution

$$\sum_{n=1}^{\infty}\binom{n}{1}\sum_{m=n}^{n+2}(-1)^{m-n}\binom{2}{m-n}\binom{m+n-2}{1}\frac{1}{(ma_1+na_2)^2} \times\left\{\Omega_2-\binom{m+n-2}{1}\Omega_3\pm\cdots\right\} \tag{17}$$

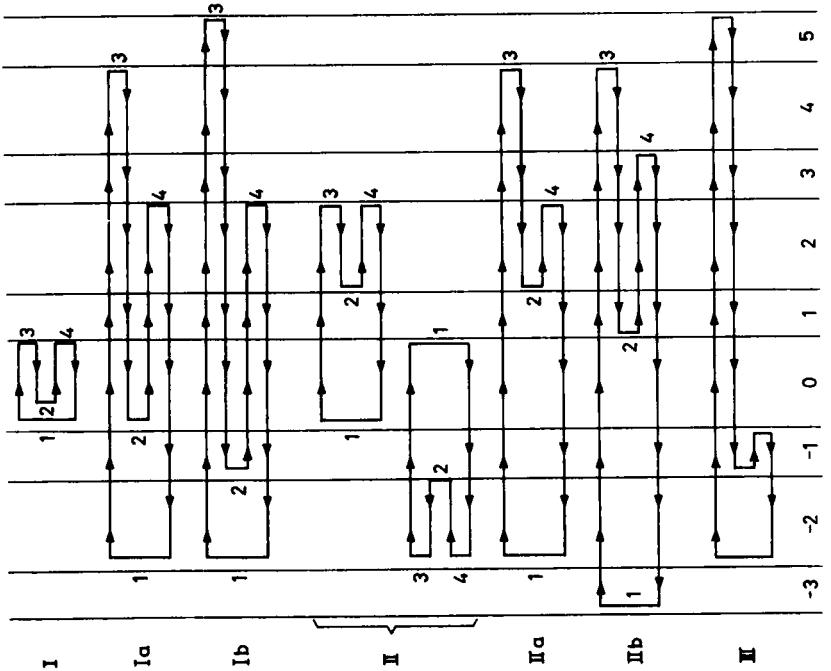

$$\frac{1}{2}\left(\frac{\varepsilon_1-\varepsilon_2}{\varepsilon_1+\varepsilon_2}\right)^4 \frac{1}{[2a_2]^2}$$

$$\frac{1}{2}\binom{n+1}{3}\left(\frac{\varepsilon_1-\varepsilon_2}{\varepsilon_1+\varepsilon_2}\right)^4 \left(\frac{-4\varepsilon_1\varepsilon_2}{(\varepsilon_1+\varepsilon_2)^2}\right)^{2n-4} \frac{1}{[(n-2)a_1+na_2]^2}$$

$$\frac{1}{2}\binom{n+1}{3}\binom{4}{m-n+2}\left(\frac{\varepsilon_1-\varepsilon_2}{\varepsilon_1+\varepsilon_2}\right)^4 \left(\frac{-4\varepsilon_1\varepsilon_2}{(\varepsilon_1+\varepsilon_2)^2}\right)^{m+n-2} \frac{1}{[ma_1+na_2]^2}$$

$$2\left(\frac{\varepsilon_1-\varepsilon_2}{\varepsilon_1+\varepsilon_2}\right)^4 \left(\frac{-4\varepsilon_1\varepsilon_2}{(\varepsilon_1+\varepsilon_2)^2}\right)^2 \frac{1}{[a_1+3a_2]^2}$$

$$2\binom{n}{3}\left(\frac{\varepsilon_1-\varepsilon_2}{\varepsilon_1+\varepsilon_2}\right)^4 \left(\frac{-4\varepsilon_1\varepsilon_2}{(\varepsilon_1+\varepsilon_2)^2}\right)^{2n-4} \frac{1}{[(n-2)a_1+na_2]^2}$$

$$2\binom{n}{3}\binom{4}{m-n+2}\left(\frac{\varepsilon_1-\varepsilon_2}{\varepsilon_1+\varepsilon_2}\right)^4 \left(\frac{-4\varepsilon_1\varepsilon_2}{(\varepsilon_1+\varepsilon_2)^2}\right)^{m+n-2} \frac{1}{[ma_1+na_2]^2}$$

$$\binom{n}{1}\binom{m+n-2}{1}\binom{2}{m-n}\left(\frac{\varepsilon_1-\varepsilon_2}{\varepsilon_1+\varepsilon_2}\right)^4 \left(\frac{4\varepsilon_1\varepsilon_2}{(\varepsilon_1+\varepsilon_2)^2}\right)^{m+n-2} \frac{1}{[ma_1+na_2]^2}$$

FIGURE 10 Paths containing four reflections

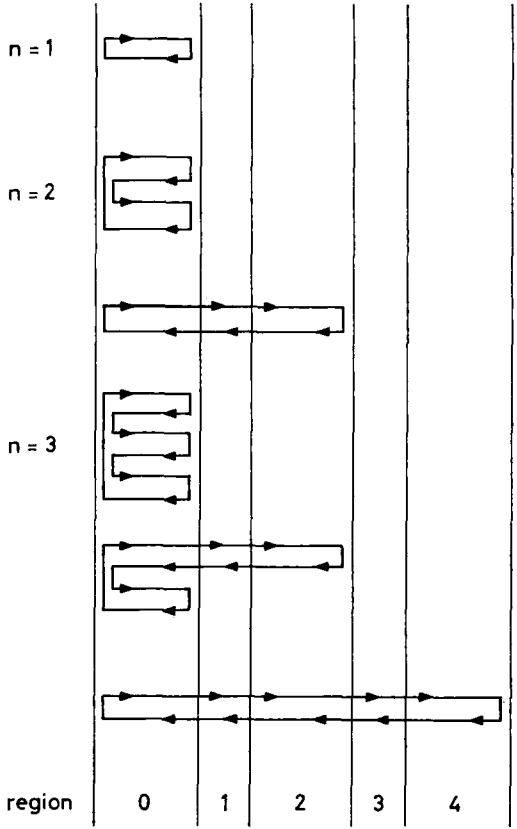

$$\sum_{i=0}^{2}\binom{2}{i}\binom{m-1}{i-1}\left(\frac{-4\varepsilon_1\varepsilon_2}{(\varepsilon_1+\varepsilon_2)^2}\right)^{i}\left(\frac{\varepsilon_1-\varepsilon_2}{\varepsilon_1+\varepsilon_2}\right)^{2m-2i+2}\frac{1}{[ma_1+a_2]^2}$$

$$\frac{1}{2}\sum_{i=0}^{4}\binom{4}{i}\binom{m-1}{i-1}\left(\frac{-4\varepsilon_1\varepsilon_2}{(\varepsilon_1+\varepsilon_2)^2}\right)^{i}\left(\frac{\varepsilon_1-\varepsilon_2}{\varepsilon_1+\varepsilon_2}\right)^{2m-2i+4}\frac{1}{[ma_1+2a_2]^2}$$

$$2\sum_{i=0}^{2}\binom{2}{i}\binom{m}{i+1}\left(\frac{-4\varepsilon_1\varepsilon_2}{(\varepsilon_1+\varepsilon_2)^2}\right)^{i+2}\left(\frac{\varepsilon_1-\varepsilon_2}{\varepsilon_1+\varepsilon_2}\right)^{2m-2i}\frac{1}{[ma_1+2a_2]^2}$$

$$\frac{1}{3}\sum_{i=0}^{6}\binom{6}{i}\binom{m-1}{i-1}\left(\frac{-4\varepsilon_1\varepsilon_2}{(\varepsilon_1+\varepsilon_2)^2}\right)^{i}\left(\frac{\varepsilon_1-\varepsilon_2}{\varepsilon_1+\varepsilon_2}\right)^{2m-2i+6}\frac{1}{[ma_1+3a_2]^2}$$

$$4\sum_{i=0}^{4}\binom{4}{i}\binom{m}{i+1}\left(\frac{-4\varepsilon_1\varepsilon_2}{(\varepsilon_1+\varepsilon_2)^2}\right)^{i+2}\left(\frac{\varepsilon_1-\varepsilon_2}{\varepsilon_1+\varepsilon_2}\right)^{2m-2i+2}\frac{1}{[ma_1+3a_2]^2}$$

$$3\sum_{i=0}^{2}\binom{2}{i}\binom{m+1}{i+3}\left(\frac{-4\varepsilon_1\varepsilon_2}{(\varepsilon_1+\varepsilon_2)^2}\right)^{i+4}\left(\frac{\varepsilon_1-\varepsilon_2}{\varepsilon_1+\varepsilon_2}\right)^{2m-2i-2}\frac{1}{[ma_1+3a_2]^2}$$

FIGURE 11 Basic paths for n = 1, 2, 3

Adding up all terms contributing integrals Ω_2 according to (13), (15), (16), (17) we obtain

$$A_{2mn} = (-1)^{m-n+2}\left\{\frac{1}{2}\binom{4}{m-n+2}\binom{n+1}{3} + 2\left[\binom{2}{m-n+2}\binom{n}{3}\right.\right.$$
$$\left.\left. + 2\binom{2}{m-n+1}\binom{n+1}{3} + \binom{2}{m-n}\binom{n+2}{3}\right]\right\} \quad (18)$$

All paths contributing to higher order integrals $\Omega_1 (l \geq 3)$ can be constructed by a similar enlarging of basic paths with characteristic positions of the reflections. We wind up with

$$A_{lmn} = (-1)^{m+l-n}\sum_{i=1} c_{li} \sum_{j=0}^{2l-2i}\binom{2l-2i}{j}\binom{2i}{m+l-n-j}\binom{n+i+j-1}{2l-1} \quad (19)$$

where the coefficients c_{li} give the number and weight of basic paths, and result recursively from

$$c_{li} = \sum_{j=1}^{i} c_{ij}\binom{l+j-1}{2i-1}; \quad c_{ll} = \frac{1}{l} \quad (20)$$

Another method of finding the coefficients A_{lmn} is by complete induction with respect to n. In this case it is convenient first to look for all basic paths with respect to the n diagrams a_2, and then to distribute the rest of diagrams a_1 to their different possible positions. The basic paths for $n = 1, 2, 3$ and their weight are shown in Figure 11. Owing to the symmetry of the two methods we find

$$A_{lmn} = A_{mln} \quad (21)$$

V DISCUSSION AND CONCLUSIONS

We start the discussion of the dispersion energy according to (12) and (19) with the limiting cases $a_1 \gg a_2$, $a_1 = a_2$, $a_1 \ll a_2$.

(a) In the case $a_1 \gg a_2$ we are left with the attraction between two half-spaces with dielectric constant ε_2. We obtain the Lifshitz formula

$$\Delta E_{AB} = -\frac{\hbar}{16\pi^2 a_2^2}\sum_{l=1}^{\infty}\frac{\Omega_l}{l^3} \quad (22)$$

(b) In the case of layers with equal thickness $a_1 = a_2$, we can carry out the summation over m and n in (12) explicitly. We obtain

$$\sum_{m,n} \frac{A_{lmn}}{(m+n)^2} = \frac{1}{l^2} \sum_{i=0}^{l-1} \frac{2^{2i} i!^2}{(2i+1)!} \sum_{j=l}^{\infty} \frac{(2j-1)!}{2^{2j} j!^2} \tag{23}$$

$$l^2 \sum_{m,n} \frac{A_{lmn}}{(m+n)^2} = \begin{cases} \log 2 & \text{for } l = 1 \\ \frac{5}{3}\left(\log 2 - \frac{1}{4}\right) & \text{for } l = 2 \\ \cdots & \\ 1 - \frac{1}{\sqrt{\pi l}} + \frac{1}{3l} \mp \cdots & \text{for } l \gg 1 \end{cases} \tag{24}$$

and

$$\Delta E_{AB} = -\frac{\hbar}{4\pi^2 (a_1 + a_2)^2} \sum_{l=1}^{\infty} \frac{\Omega_l}{l^2} \left(1 - \frac{1}{\sqrt{\pi l}} + \frac{1}{3l} \mp \cdots\right) \tag{25}$$

The contribution of the first order reflections 1 = 1 to the dispersion energy between multilayers of equal thickness is reduced by a factor of log 2, compared to their contribution to the dispersion energy between half-spaces. This is due to the repulsive reflections at the rear interfaces f_{nn+1}, n = 1, 3, 5, . . . and $n = -2, -4, -6, \ldots$ The contributions of the higher order reflections $l \geq 2$, on the other hand, are increased by a factor of l due to their increased number.

(c) The enhanced importance of the higher order reflections becomes even more pronounced in the case $a_1 \ll a_2$, that is in the case of attraction between thin films. Expanding $(ma_1 + na_2)^{-2}$ in (12) into a Taylor series with respect to $a_1/(a_1 + a_2)$, we find the largest not mutually cancelling terms to result from those paths, which cross no region a_2 twice, but are repeatedly reflected within regions a_1. These paths contribute to the terms $i = 1$ in A_{lmn} according to (19). Using $c_{l1} = l$ we obtain

$$\Delta E_{AB} = -\frac{\hbar}{16\pi^2} \zeta(3) \left\{ \frac{3! a_1^2}{(a_1 + a_2)^4} \sum_{l=1}^{\infty} l\Omega_l - \frac{4! a_1^3}{(a_1 + a_2)^5} \sum_{l=2}^{\infty} l(l-1)\Omega_l^{\pm} \pm \cdots \right\} \tag{26}$$

where $\zeta(n)$ is Riemann's zeta function, $\zeta(3) = \Sigma\, 1/n^3 = 1.202057$.

The dispersion energy between films increases quadratic with their thickness a_1, and is inversely proportional to the fourth power of their separation a_2. The dielectric factor $\Sigma l\Omega_l$ can be summed exactly to give

$$\sum_{l=1}^{\infty} l\Omega_l = \int_{-\infty}^{+\infty} d\omega \left(\frac{(\varepsilon_1 - \varepsilon_2)(\varepsilon_1 + \varepsilon_2)}{4\varepsilon_1\varepsilon_2} \right)^2 \tag{27}$$

Compared to the essential integral Ω_1 for the attraction between half-spaces, we find the importance of the extremum regions of ε_1, ε_2 increased considerably. The integrand in (27) approaches $(\varepsilon_1/4\varepsilon_2)^2$ for $\varepsilon_1 \gg \varepsilon_2$, while the equivalent integrand in Ω_1 merely approaches 1.

The increasing importance of the higher order reflection terms with decreasing layer thickness a_1 causes the dispersion energy to be of longer range than expected from a pairwise integration of d^{-6} interactions. This result, which was first reported by Ninham and Parsegian[5], is in agreement with the general rule that adsorbate layers dominate the dispersion energy between solids at separations smaller than the layer thickness[2,3]. The dispersion energy between multilayers is primarily determined by the dielectric properties of regions ± 1 for $a_2 < a_1$, whereas the dielectric properties of regions ± 2 become important only if $a_2 > a_1$.
Computed results on

$$I_l\left(\frac{a_1}{a_1 + a_2}\right) = \sum_{m,n} \frac{A_{lmn}}{\left(m \dfrac{a_1}{a_1 + a_2} + n \dfrac{a_2}{a_1 + a_2} \right)^2} \tag{28}$$

for $l = 1, 2, \ldots, 20$ are summarized in Figure 12. In addition to the verification of the limiting laws (22), (25) and (26), we find the coefficients I_l with $l \geq 5$ not to decrease monotonic with $a_1/(a_1 + a_2)$, but to assume extremes. The position of the minima tends towards $a_1/(a_1 + a_2) = 1/2$, which means that (25) is correct in a relatively broad region. The position of the maxima, on the other hand, tends towards $a_1/(a_1 + a_2) = 0$. This region is shown enlarged in Figure 13. I_l assumes its maximum approximately at $a_1/(a_1 + a_2) = 1/l$. From Figs. 12 and 13 it is obvious that the different I_l-curves approach an envelope, which for $a_1/(a_1 + a_2) < 0.2$ is approximately given by

$$\text{envelope } \{I_l\} \simeq 0.75 \frac{a_1}{a_1 + a_2} + 2\left(\frac{a_1}{a_1 + a_2}\right)^2 + \cdots \tag{29}$$

The monotonic decrease of the dielectric integrals Ω_l with increasing l makes it very unlikely that the extremes of the coefficients I_l with respect to a_1 are carried over to the dispersion energy. Representing the latter in the

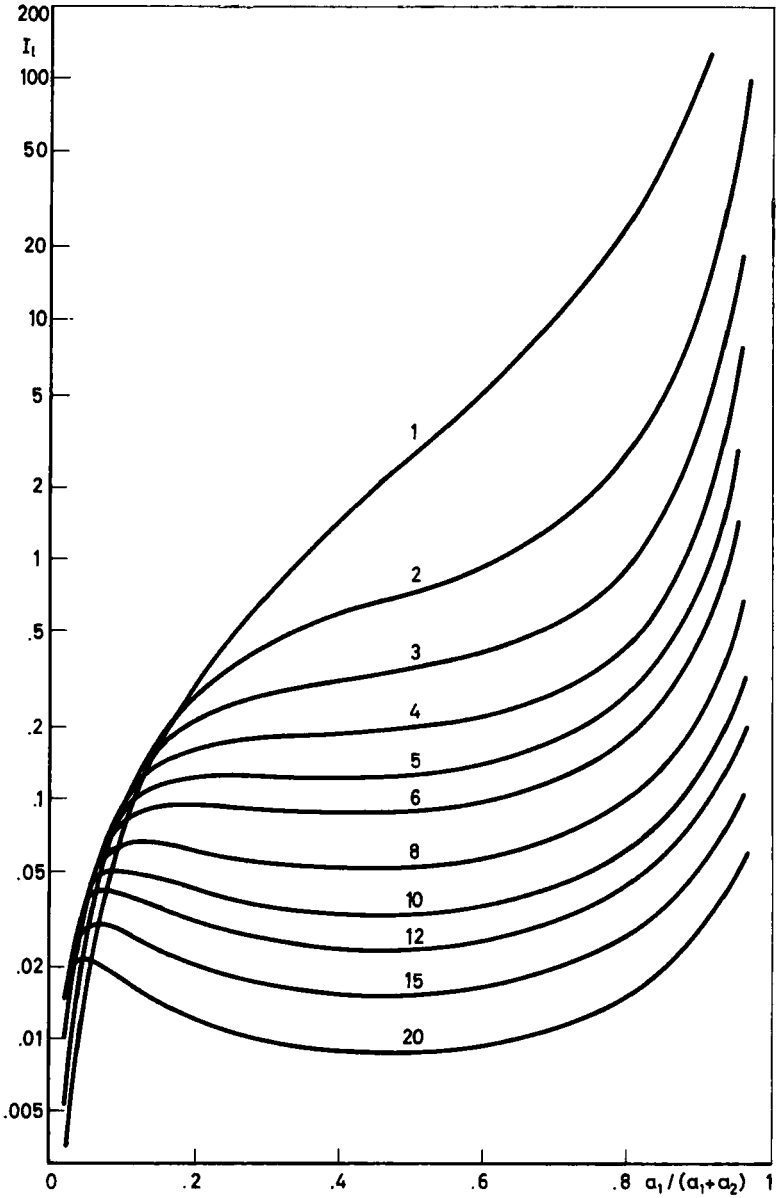

FIGURE 12 Computed coefficients I_l

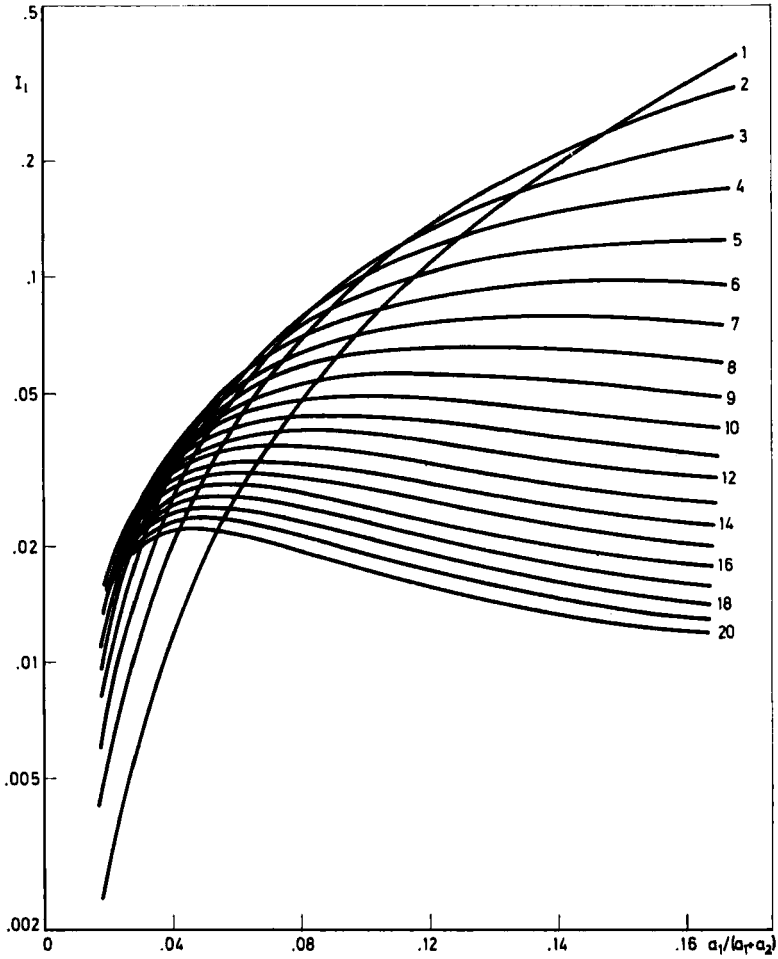

FIGURE 13 Computed coefficients I_1

form

$$\Delta E_{AB} = -\frac{\hbar}{16\pi^2(a_1 + a_2)^2} \sum_{l=1}^{\infty} I_l \Omega \tag{30}$$

we find the behavior of ΔE_{AB} in the region $a_1 < a_2$ largely governed by that of the envelope (29). In order to demonstrate the increase in range of ΔE_{AB} resulting from the reflection terms $l \geq 2$, we plotted $\Delta E_{\text{multilayer}}/\Delta E_{\text{half-spaces}}$ versus a_2/a_1 in Figure 14. For reasons of simplicity, we replaced the monotonic decrease of the dielectric integrals Ω_l by an abrupt change from 1 to 0.

The parameter of the different curves in Figure 14 is the number L, where the dielectric integrals are cut off, $\Omega_l = 1$ for $l \leq L$, $\Omega_l = 0$ for $l > L$. The case $L = 1$ corresponds to the behavior resulting from a pairwise integration of d^{-6} interactions. The increase in the range of attraction with increasing L is obvious. The dashed line is the dispersion energy between half-spaces ($a_2/a_1 = 0$). The dotted line in Figure 14 is the result obtained by Ninham and Parsegian[5] for the dispersion energy between hydrocarbon-water layers. From the fact that this line lies amidst the curves $L = 1, \ldots, 5$ for medium separations, but above the curves $L = 1, \ldots, 5$ for large separations, we conclude that agreement of both treatments is obtained if instead of abruptly cutting off the dielectric integrals we assume a more realistic behavior like $\Omega_l = x^{l-1}$ with $x < 1$. Explicit investigations on the dielectric integrals Ω_l in different media and on the resulting behavior of the dispersion energy in multilayers will be reported in a subsequent paper.

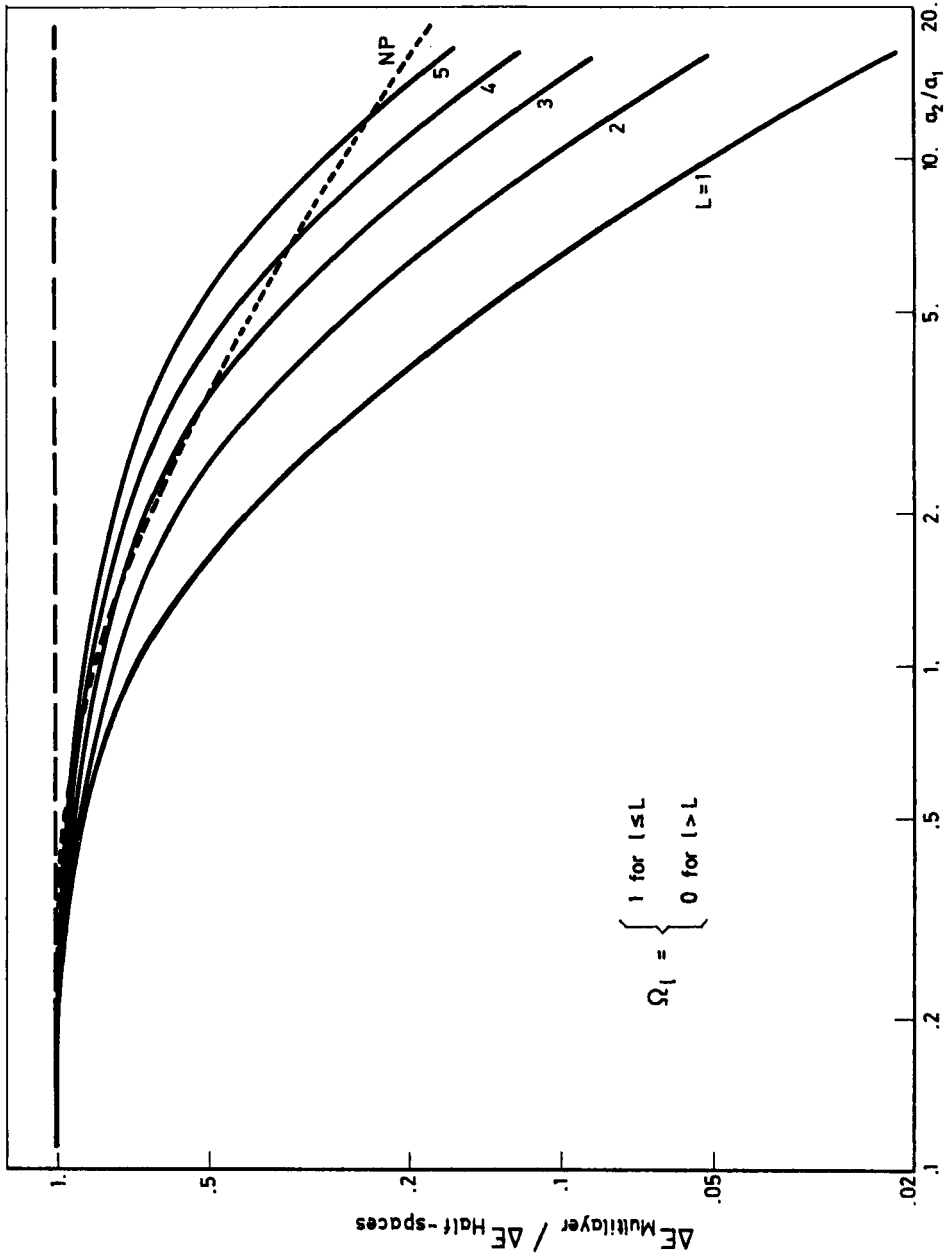

FIGURE 14 Dispersion energy versus reduced separation

References

1. D. Langbein, *J. Phys. Chem. Solids* **32,** 133 (1971).
2. D. Langbein, *J. Adhesion* **1,** 237 (1969).
3. D. Langbein, *J. Phys. Chem. Solids* **32,** 1657 (1971).
4. B. W. Ninham and V. A. Parsegian, *J. Chem. Phys.* **52,** 4578 (1970).
5. B. W. Ninham and V. A. Parsegian, *J. Chem. Phys.* **53,** 3398 (1970).
6. E. M. Lifshitz, *Zh. Eksperim. i Teor. Fiz.* **29,** 94 (1955), [*Soviet Phys. JETP* **2,** 73 (1956)].
7. I. E. Dzyaloshinskii, E. M. Lifshitz and L. P. Pitaevskii, *Zh. Eksperim. i Teor. Fiz,* **37,** 229 (1956), [*Soviet Phys. JETP* **37** (10), 161 (1960)].